Materials Today Communications 21 (2019) 100613

Contents lists available at ScienceDirect

Materials Today Communications

journal homepage: www.elsevier.com/locate/mtcomm

Short communication: Assessment of the dislocation density using X-ray topography in Al single crystals annealed for long times near the melting temperature

S.P. Singh[a], X-R. Huang[b], P. Kumar[a], M.E. Kassner[c,*]

[a] Department of Materials Engineering, Indian Institute of Science, Bangalore, 560012, India
[b] Advanced Photon Source, Argonne National Laboratory, Argonne, IL, 60439-4800, USA
[c] Department of Chemical Engineering and Materials Science, University of Southern California, Los Angeles, CA, USA

ARTICLE INFO

Keywords:
Annealing
Dislocation density
X-ray topography

ABSTRACT

Earlier work by the authors determined the dislocation density as a function of time in aluminum single crystals annealed near the melting temperature using etch-pits. It was found that the dislocation density is stable and unchanged even with annealing times up to one year for statically annealed Al single crystals with an initially low dislocation density. As several investigators have suggested that etch-pits are not reliable compared to transmission electron microscopy in assessing the dislocation density, the current study utilized x-ray topography at a synchrotron for dislocation density measurements. This work, then, is a short paper complementing the authors earlier work by using a new, reliable, but rarely utilized non-destructive technique to measure the dislocation density. The results confirm the trend of the earlier study using etch-pits by the authors.

1. Introduction

The authors of this work found that the dislocation density in single crystal aluminum is stable after one year of annealing at $0.98T_m$, where T_m is the melting temperature of material, based on etch-pits to identify the dislocations [1]. This is illustrated in Fig. 1. The dislocation density is remarkably stable at about $10^9\,m^{-2}$. Dislocation density determination by etch-pits, however, has been suggested to be inaccurate in [2–4]. Two of these works ([2,4]) suggested that etch-pits were less reliable than dislocation density measurements by transmission electron microscopy (TEM). However, determination of low dislocation densities by TEM was questioned by Nes [5]. He suggested that typically 100 foils will be required to characterize a single dislocation for dislocation densities less than $10^9\,m^{-2}$. The authors of this work believe that at the low dislocation densities observed in these studies, slight damage in TEM thin foil preparation appeared to give false assessments of the dislocation density [6]. An additional technique that appears fully reliable is x-ray topography that was successfully used by Nes and Nost for Al single crystals [7]. This procedure of characterizing and measuring dislocation density is quite common amongst the crystal growth community; however, it has been scarcely used by metallurgists considering that the x-ray topography is not ideal for measuring dislocation density in excess of $10^{10}\,m^{-2}$. Since we expect dislocation density in samples of interest in this work to be less than $10^{10}\ m^{-2}$, we utilized x-ray topography at the Advance Photon Source (APS) synchrotron at Argonne National Laboratory, Illinois, USA.

2. Experimental procedure

High purity Al single crystals of (111) orientation and 99.999% and 99.9999% purity were obtained from MaTeck Material-Technologie & Kristalle GmbH, Juelich, Germany. These crystals were annealed at 920 K ($\sim 0.98\ T_m$) for various times up to 1 year. The details of sample preparation and annealing technique are described in [6].

X-ray topography for dislocation density determination after various annealing times was conducted using white beam from a synchrotron at 1-BM Beamline with 7 GeV capacity at the Advanced Photon Source (APS), at Argonne National Laboratory. The white incident beam consisted of an energy spectrum ranging from 6 keV to energies of > 100 keV and wavelengths ranging from 1 pm to 10 nm. The wide spectrum of wavelengths provides an excellent tolerance to the regions with different orientations and deformation. On the other hand, low horizontal and vertical divergences, small source size and long source-specimen distance provide excellent resolution for imaging [8,9]. These make usage of X-ray topography for measuring dislocation density quite reliable. The imaged specimens were the same as those of the authors'

* Corresponding author.
E-mail address: kassner@usc.edu (M.E. Kassner).

https://doi.org/10.1016/j.mtcomm.2019.100613
Received 24 June 2019; Received in revised form 20 August 2019; Accepted 20 August 2019
Available online 07 September 2019

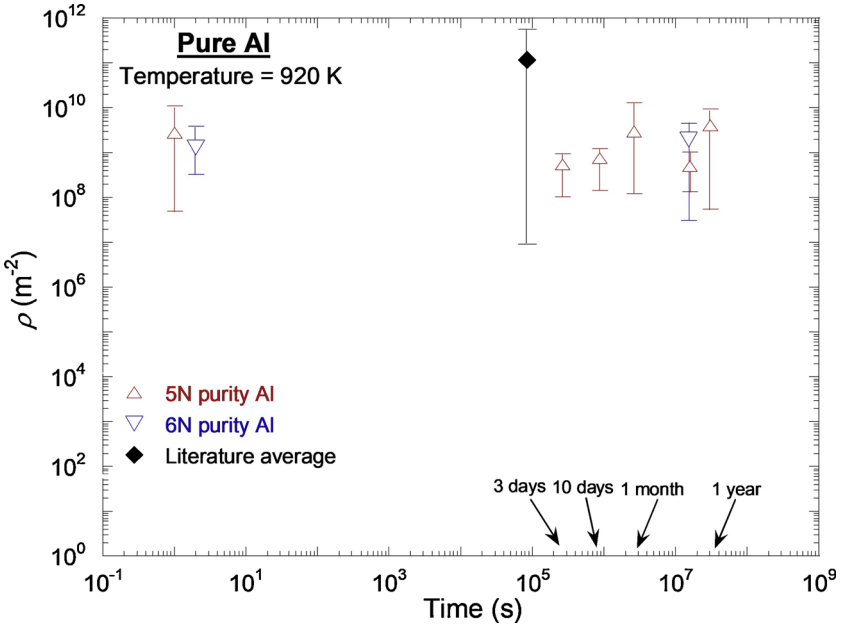

Fig. 1. The dislocation density (determined by etch-pits) versus annealing time at 920 K from authors' earlier work [1].

earlier work recently published in ref [1].

X-ray topography of the samples was conducted using a reflection geometry. This grazing angle reflection geometry is illustrated in Fig. 2. Samples of 25.4 mm diameter and 6 mm thickness were placed on an aluminum stage mounted on a goniometer. The samples were tilted using the goniometer at an angle of 4° with respect to the incident white beam as shown in Fig. 2. 200 mm × 250 mm x-ray films were used to capture the Laue patterns produced by the incident white beam. The exposure time of white beam on the sample was varied from 100 to 500 ms. These films were placed at 120 mm from the sample and tilted at 28.5° from the vertical direction. Laue patterns were captured on the x-ray films. Subsequently, the Laue spots were observed under an optical microscope under transmission mode and digitized to capture the images showing the dislocation structure (see Fig. 3). The images were captured at a magnification of 40X in the optical microscope. X-ray films used to capture the images had limited spatial resolution. Capturing images at higher magnification makes it appear blurry. This restricts the resolution of the captured images. Hence, a very high-resolution image could not be obtained in the present study.

The dislocation density was calculated as [10],

$$\rho = \frac{2N}{Lt} \tag{1}$$

where N is the number of intersections of dislocations with the randomly drawn lines, L is the total line length and t, in the present case of topography, is the average information or penetration depth of the white beam. For example, the solid dots in magnified view of Fig. 3b show the points where a randomly drawn line (of length L_i) intersects the dislocations and their total number is assigned a value of N_i for the particular line. In practice, several such lines were drawn over a set of high magnification images, and an overall average value of N_i/L_i was calculated to be used in Eq. (1). For an accurate determination of dislocation densities using x-ray topography technique, it is important to estimate the penetration depth of the x-rays, as assessed by [11],

$$G_x = 1 - e^{-\mu x\left(\frac{1}{\sin\alpha}+\frac{1}{\sin\beta}\right)} \tag{2}$$

where G_x is the fraction of the total intensity captured (on x-ray film) relative to the incident beam, μ is the linear absorption coefficient, x is the depth of penetration, α and β are the incidence and reflectance angle, respectively, as shown in Fig. 2. The penetration depth in the case of a monochromatic beam can be calculated with reasonable

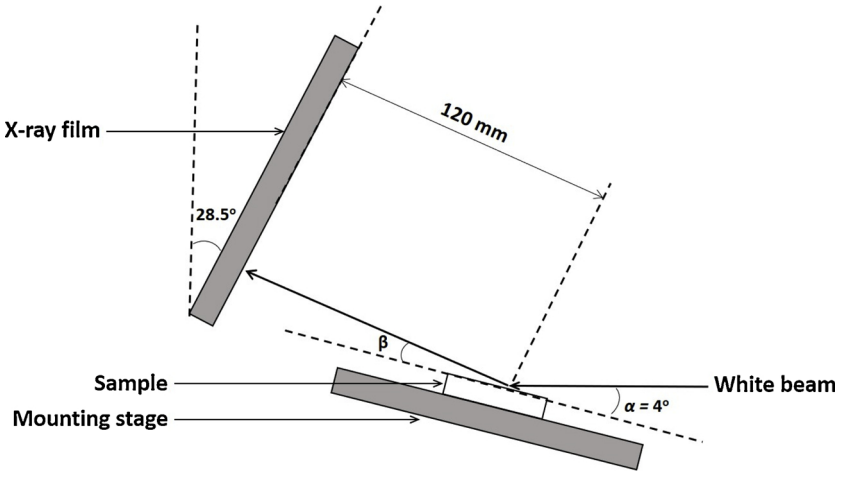

Fig. 2. Schematic illustration of the experimental setup used for x-ray topography.

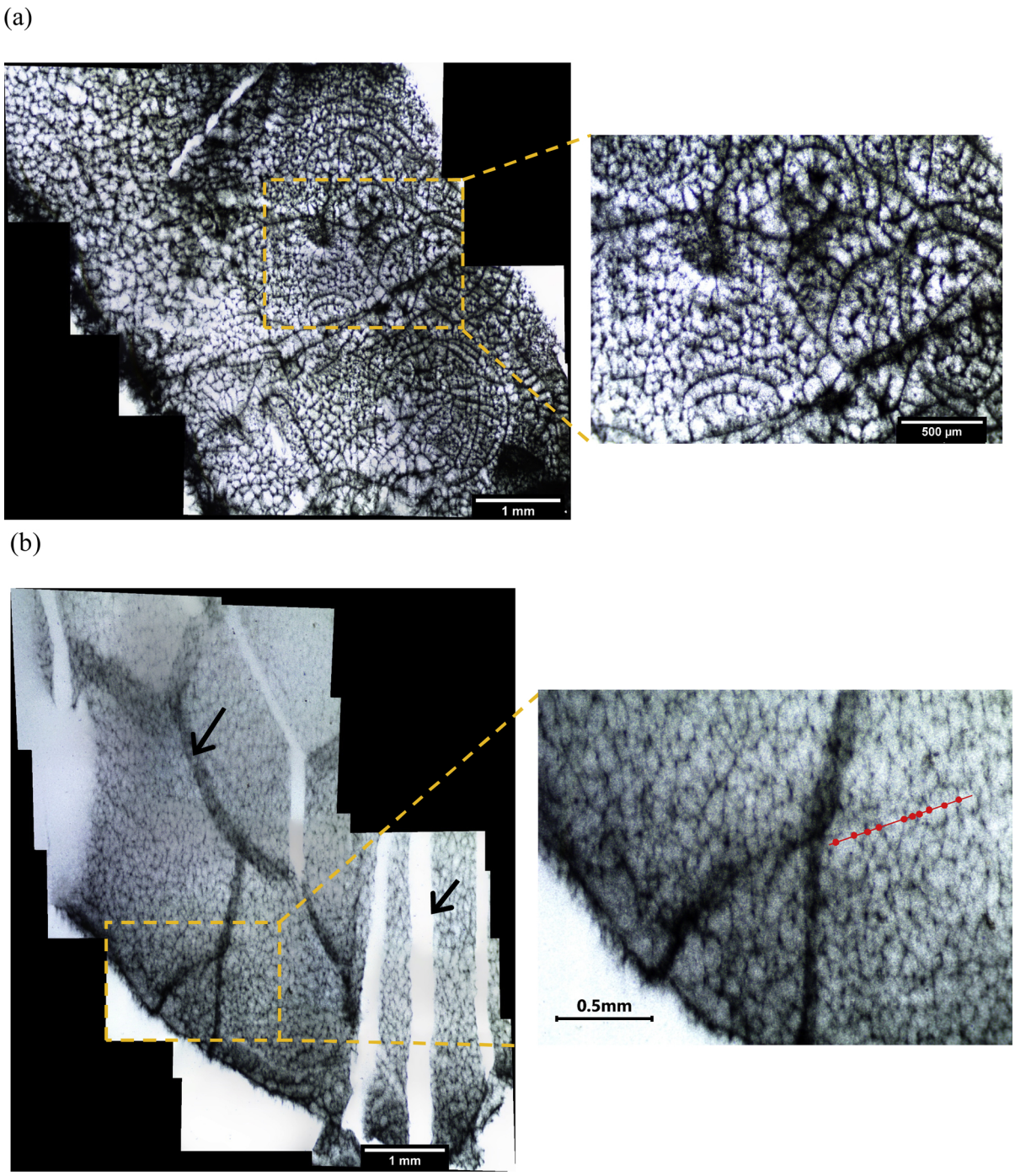

Fig. 3. Topographs showing dislocation structure in, (a) as-received and (b) 1-month annealed Al (111) single crystals. Inset in each figure show magnified view of the regions bounded by the broken squares. A random line is drawn in inset of (b), wherein the solid dots indicate the point of intersection of this line with dislocation lines. The arrows in (b) delineate boundaries associated with, in the present case, small misorientations.

accuracy using the values of the μ, α and β. However, the calculation of penetration depth is not straightforward in the case of white beam radiation which consists of a wide spectrum of wavelengths leading to different values of β for the diffracted beam. The value of μ also depends upon the incident photon energy which is a spectrum in case of white beam.

Here, LauePt software [12] was used to index the obtained Laue diffraction patterns from the (111) oriented Al single crystals. The topographs shown in Fig. 3 are obtained from a $(\bar{1}0\bar{3})$ reflection. This reflection corresponds to a 0.725 Å wavelength, which has a photon energy of 16.4 keV. The variation of absorption coefficient, μ, with photon energy can be obtained from NIST tables for mass absorption coefficients which is 17.7 cm^{-1} for 16.4 keV [13]. α was set to 4° and β varied from 4 to 6°. The average information depth or effective penetration depth, t, which is defined as the center of gravity of distribution between the diffracted intensity and the depth, is usually assessed as the distance by which the intensity falls by a factor of 1/e. Hence, if G_x in Eq. (2) is considered to be (1- 1/e), then the following expression can be derived for the effective penetration depth [14]:

$$t = \frac{\sin\alpha \sin\beta}{\mu(\sin\alpha + \sin\beta)} \quad (3)$$

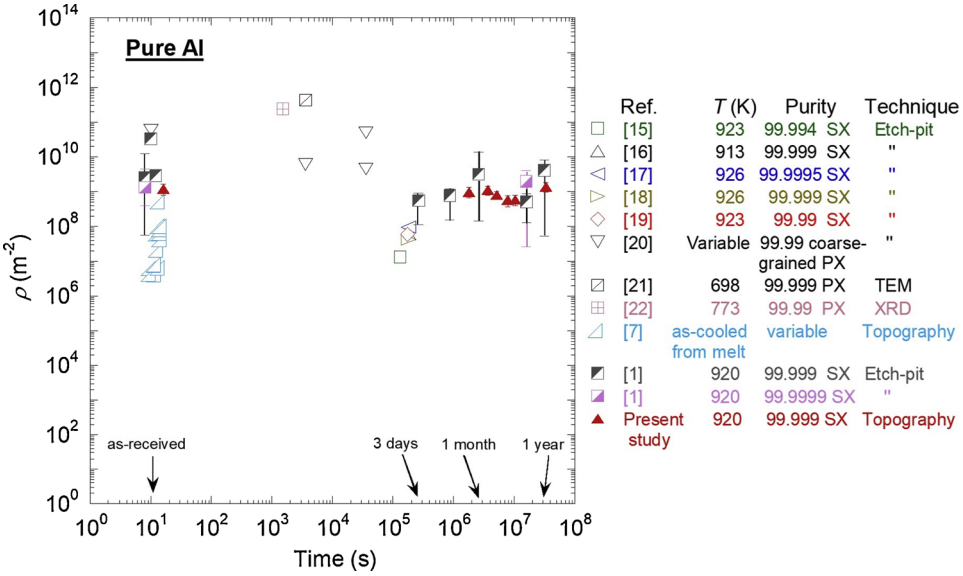

Fig. 4. The etch-pit and x-ray-topography-based dislocation density measurements as a function of annealing time at 920 K ($0.98T_m$). SX refers to single crystals and PX refers to polycrystalline specimens [15–18,20–22].

Given the values of α and β for the observed $(\bar{1}0\bar{3})$ reflection in this study, Eq. (3) yields a value of the effective penetration depth as 24 ± 7 μm. This can be used in Eq. (1) to estimate the dislocation density. The calculated dislocation densities are shown in Fig. 4. The error bar in Fig. 4 corresponds to the uncertainty related to the measurement of the effective penetration depth. In practice, the dislocation densities assuming penetration depths of 17, 24 and 31 μm were calculated and the standard deviation obtained for these 3 penetration depths was plotted as an error bar in Fig. 4. It is important to note here that the above calculation for effective penetration depth only assumes the dominant operative wavelength and hence there might be a larger spread in the dislocation density as compared to that shown using the error bars in Fig. 4. It should be noted that there is no magnification involved in topography [8].

3. Results and discussion

The dislocation structure obtained from white beam topography is shown in Fig. 3. Fig. 3a shows the dislocation structure in as-received Al single crystal. A Frank network of dislocations appears to be observed. Fig. 3b shows the dislocation structure in 1-month annealed Al single crystal at 920 K. A few white and dark bands are indicated by arrows in Fig. 3b. It should be noted that the images shown in Fig. 3 are individual dislocations rather than a dislocation cell development. This is consistent with the etch-pit analysis that show no evidence of cell development [1]. The images in Fig. 3 represent a Frank dislocation network, that could be confused with cell wall development. These regions of white and dark bands correspond to local misorientations in the lattice presumably from low-angle boundaries which probably developed with high temperature annealing [8]. The typical misorientation calculated from bands indicated by arrows in Fig. 3b is 0.06 ± 0.02°. It should be noted that the reported dislocation density does not include dislocations associated with these boundaries. The formation of these boundaries suggests a decrease in the dislocation density with annealing, although a constant value of this network density appears to be achieved.

Fig. 4 illustrates the dislocation densities as a function of time. The results suggest that a decrease of a factor of two or, so, in the total dislocation density from the as-received crystal may occur with the achievement of a constant minimum value. Fig. 4 clearly reveals that the topography measurements of the dislocation densities are comparable to those determined by etch-pits of the authors' earlier study. Also, the topography assessment is consistent with the earlier conclusion that the dislocation density becomes invariant with annealing time.

The basis for the frustration of the network is unclear. Ardell et al. [19,23] suggested that this occurs as a result of the requirement that the nodes must obey Franks rule which may preclude coarsening. Nabarro suggests that a Peierls stress basically pins the dislocations of the network at very low stresses precluding coarsening [24]. The authors will discuss this issue in a subsequent publication.

4. Conclusions

Aluminum single crystals were annealed at $0.98T_m$ for times up to one year. The dislocation density as a function of annealing time was evaluated using x-ray topography. The topography measurements of the dislocation densities are comparable to those determined by etch-pits of an earlier study by the authors which showed that the dislocation density becomes invariant with annealing times even after one year at the very high annealing temperature.

Acknowledgements

Research at the University of Southern California was supported the National Science Foundation through DMR-1401194. SPS and PK would like to thank IISc for partial support (travelling to USC). The facilities on the 1-BM beamline at the APS are supported by the DOE Office of Science under Contract No. DE-AC02- 06CH11357.

References

[1] K.K. Smith, M.E. Kassner, P. Kumar, Long-term annealing of high purity aluminum single crystals: new insights into harper-dorn creep, Mater. Sci. Eng. A-Struct. 705 (2017) 1–5.
[2] P. Yavari, D. Miller, T.G. Langdon, *An investigation of harper-dorn creep- mechanical and microstructural* characteristics, Acta Metall. Mater. 30 (1982) 871–879.
[3] G. Meyrick, On the dislocation density in aluminum during harper-dorn creep, Scripta Metall. Mater. 23 (1989) 2025–2028.
[4] A.J. Forty, F.C. Frank, The interpretation of etch patterns on aluminum, J. Phys. Soc. Jap. 10 (1955) 656–663.
[5] E. Nes, Modeling of work hardening and stress saturation in FCC metals, Prog. Mater. Sci. 41 (1998) 129–193.
[6] K. Smith, Ph D. Thesis, Dept. of Chemical Engineering and Materials Science, University of Southern California, 2017.
[7] E. Nes, B. N∅st, Dislocation densities in slowly cooled aluminum single crystals,

Philos. Mag. 124 (1966) 855–865.
[8] B. Raghothamachar, G. Dhanaraj, J. Bai, M. Dudley, Defect analysis in crystals using X-ray topography, Microsc. Res. Techniq. 69 (2006) 343–358.
[9] A. Macrander, M. Erdmann, N. Kujala, S. Stoupin, S. Marathe, X. Shi, M. Wojcik, et al., X-ray optics testing beamline 1-BM at the advanced photon source, AIP Conf. Proc., AIP Publishing (2016) 1741 030030.
[10] R.K. Ham, The determination of dislocation densities in thin films, Philos. Mag. 6 (1961) 1183–1184.
[11] B.D. Cullity, Elements of X-Ray Diffraction, (2001), pp. 269–272.
[12] X.R. Huang, LauePt, a graphical-user-interface program for simulating and analyzing white-beam X-ray diffraction Laue patterns, J. Appl. Crystallogr. 43 (4) (2010) 926–928.
[13] https://physics.nist.gov/PhysRefData/XrayMassCoef/ElemTab/z13.html, accessed on May 15, 2019.
[14] U. Welzel, J. Ligot, P. Lamparter, A.C. Vermeulen, E.J. Mittemeijer, Stress analysis of polycrystalline thin films and surface regions by X-ray diffraction, J. Appl. Crystallogr. 38 (2005) 1–29.
[15] C.R. Barrett, E.C. Muehleisen, W.D. Nix, High temperature-low stress creep of Al and Al+ 0. 5% Fe, Mater. Sci. Eng. 10 (1972) 33–42.
[16] P. Kumar, Ph.D. Thesis, Dept. of Chemical Engineering and Materials Science, University of Southern California, 2007.
[17] T.J. Ginter, F.A. Mohamed, Evidence for dynamic recrystallization during Harper–Dorn creep, Mater. Sci. Eng. A-Struct. 322 (2002) 148–152.
[18] F.A. Mohamed, T.J. Ginter, On the nature and origin of Harper-Dorn creep, Acta Metall. Mater. 30 (10) (1982) 1869–1881.
[19] S. Lee, A.J. Ardell, Dislocation link length distributions during Harper-dorn creep of monocrystalline aluminum, Strength of Metals and Alloys (ICSMA 7), Pergamon, 1985, pp. 671–676.
[20] B.Y. Pines, A.F. Syrenko, Change of dislocation density in aluminium and lithium fluoride after annealing near the melting point under hydrostatic pressure, J. Mater. Sci. 3 (1) (1968) 80–88.
[21] M.E. Kassner, M.E. McMahon, The dislocation microstructure of aluminum, Metall. Mater. Trans. A 18 (5) (1987) 835–846.
[22] G.K. Williamson, W.H. Hall, X-ray line broadening from filed aluminium and wolfram, Acta Metall. Mater. 1 (1) (1953) 22–31.
[23] A.J. Ardell, Harper–Dorn creep–The dislocation network theory revisited, Scripta Metall. Mater. 69 (7) (2013) 541–544.
[24] F.R.N. Nabarro, Creep at very low rates, Metall. Mater. Trans. A 33 (2) (2002) 213–218.